



Striation Formation in Ti-doped $Y_3Al_5O_{12}$ Fibers Grown by the Laser Heated Floating Zone Method

T. KOTANI*, J.K.W. CHEN** & H.L. TULLER

Crystal Physics and Electroceramics Laboratory, Department of Materials Science and Engineering, Massachusetts Institute of Technology, Cambridge, MA 02139, USA

Submitted May 20, 1997; Revised January 16, 1998; Accepted January 27, 1998

Abstract. Microscopic dopant distribution has been investigated in 1 mm-diameter single crystal fibers of Ti-doped $Y_3Al_5O_{12}$ (YAG) grown by a laser heated floating zone (LHFZ) method. In the fibers, a periodic fluctuation in the Ti dopant concentration has been observed along the growth direction, and striations, attributed to variation in dopant concentration, were seen across the diameter of the fiber by two dimensional mapping using an electron probe microanalyser. The dopant concentration was found to vary by as much as 30% from average levels with a spacing of the order of 20 μm . Microscopic inhomogeneities of Ti are discussed in relation to growth conditions with emphasis on crystal/feed rotation. Effects to minimize segregation effects by annealing are reported.

Keywords: YAG, striation, floating zone, dopant, single crystal fiber growth, $Y_3Al_5O_{12}$, diffusion

1. Introduction

Single crystal fibers of oxides are being extensively studied as laser materials [1] and reinforcements for high temperature composites [2,3]. We are interested in employing single crystal fibers for characterization of electrical, optical and defect properties of YAG doped with Ti, Cr or Zr [4,5]. For these purposes, well-defined doping is needed to reproducibly control the mechanical, electrical and optical properties of the doped YAG fibers. However, one may find nonuniform dopant-distribution in grown fibers due to nonunity segregation coefficients and evaporative loss of dopants. We have reported, for example, nonuniform distribution of dopants on a macroscale along Ti- and Cr-doped YAG fibers grown by a laser heated floating zone method [6]. These inhomogeneities could be related to atmosphere-dependent segregation coefficients and evaporative loss of dopants, both of which are connected to the variable

valent nature of the dopants [6]. It is also important to investigate microscopic dopant inhomogeneities like striations, which are commonly observed in crystals grown by the Czochralski method. In this study, we address striation formation in Ti-doped YAG fibers in relation to growth conditions, with emphasis on crystal/feed rotation.

2. Experimental

2.1. Fiber Growth

Fibers with approximately 1 mm diameter were grown by the LHFZ growth method. This technique is a crucible-free method with a cold wall and provides flexibility in controlling the growth atmosphere. In addition, it enables one to grow heavily doped crystals at a relatively high growth rate without constitutional supercooling, taking advantage of the steep temperature gradient near the growth interface. Two kinds of laser heated floating zone growth systems equipped with a 2-beam 100 W or a 4-beam 1.5 kW CO_2 laser, shown in Fig. 1, were employed for the fiber growth.

* Permanent address: Basic High-Technology Laboratories, Sumitomo Electric Industries, Ltd., 1-1-3 Shimaya, Konohana-ku, Osaka 554, JAPAN

** Permanent address: Form Factor, Inc., 5666 La Ribera St., Livermore, CA 94550, USA

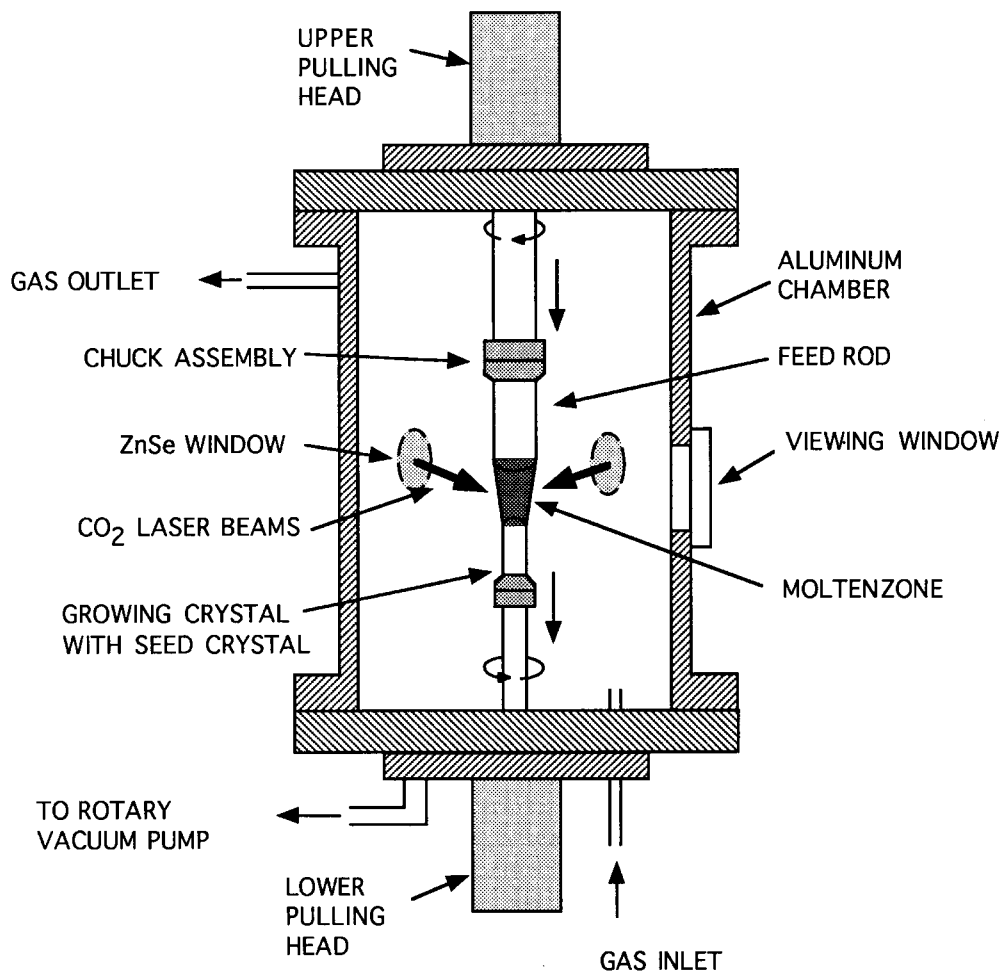


Fig. 1. Schematic diagram of the LHFZ (laser heated floating zone) growth apparatus.

Polycrystalline source materials, with compositions of $Y_3(Al_{1-x}Ti_x)_5O_{12}$ ($x=0, 0.05$), were typically employed as feed rods. A modified Pechini process was used to make YAG powder. This process employs citric acid solutions of Y and Al, as well as dopants, which are mixed together in the appropriate ratios for the desired composition. The solution is then dried, ashed in flowing O_2 at $\approx 600^\circ C$, and then calcined to the oxide phase at $\approx 900^\circ C$. The detailed preparation procedure is described elsewhere [5]. All powders were confirmed to be single phase using X-ray diffraction. The powders were then pressed into pellets and sintered in vacuo at $1800^\circ C$ for 2 h. The feed rods were cut from the pellets with square cross sections with typical dimensions of $1\text{ mm} \times 1\text{ mm} \times 15\text{ mm}$.

Fibers were grown either by using uniformly doped polycrystalline feed rods, or a combination of undoped YAG single-crystal rods with uniform diameter and TiO_2 single crystals. In the latter case, a two-step procedure, including doping and fiber-growth steps, was used. Prior to fiber growth, a TiO_2 source rod was contacted to the molten end of the undoped YAG single crystal rod. The TiO_2 rod was then switched to a YAG seed crystal as in the first case. This procedure was employed to examine the solubility and segregation of Ti into the YAG fibers since the concentration decreases monotonously with growth length. Typical growth conditions are summarized in Table 1. In all cases, the molten zone traversed the length of the fiber only once. The crystal rotation rate was varied during growth, in a number of

Table 1. Summary of typical growth conditions

| | |
|-----------------------|--|
| Growth rate: | 2 cm/h, downward |
| Growth orientation: | [111] Undoped or lightly Ti-doped seed crystal |
| Rotation(fiber/feed): | 0 or 21 rpm (CW)/16 rpm (CCW) for 2-beam system 12 rpm (CW)/9 rpm (CCW) for 4-beam system |
| Zone length: | 1.5–2.9 mm |
| Atmosphere: | After evacuation to 30–50 mTorr, backfilled with Ar or Ar + 5% H ₂ gas to 1 atm |
| Crystal dimensions: | 0.9–1.4 mm in diameter, 10–40 mm long |

growth runs, to investigate its influence on striation formation. Grown YAG fibers showed Ti concentration up to $x = 0.05$ for $Y_3(Al_{1-x}Ti_x)_5O_{12}$.

2.2. Electron Probe Microanalysis (EPMA)

Quantitative analyses were performed at intervals of 4–10 μm both along the growth direction and across the diameter of the fibers using electron probe microanalysis (EPMA). Measurements were performed with a JEOL Superprobe 733, operating with a beam diameter of 1 μm , a beam current of 10–20 nA and a voltage of 15 kV using YAG and TiO_2 as standards. Ti concentrations are expressed as a cation percentage of Al sites in the $Y_3Al_5O_{12}$ lattice. Typical detection limits of the analyses were approximately 0.1%.

Semi-quantitative 2-D maps of Ti distributions in the fiber cross section were made by means of Shimadzu EPMA 8705 Q2H3, operating with an electron beam diameter of 1 μm at 15 kV and 50 nA. The intensity of the characteristic X-ray of Ti was measured on the whole cross section with steps of 10 μm . Prior to analysis, all fibers were polished flat along the growth direction with 12 μm , 1 μm and 0.05 μm alumina abrasives using a conventional polishing jig and machine. Polished slices with (111) surfaces were also employed for analysis of radial Ti distribution. The surface of the specimens was then coated with a 250 \AA thick carbon film to prevent charge-up induced by the electron beam during analysis. All specimens selected for analysis were precipitate free.

3. Results and Discussion

Typical macroscopic and microscopic variations of Ti along the growth direction are shown in Fig. 2. The periodicity of the dopant fluctuation was observed to be on the order of 20 μm . The concentration variation was found to vary by as much as 25–30% from the average concentration. As the growth interface was typically convex towards the melt as observed in the frozen molten zone [6], radial variation in dopant concentration was also observed across the diameter of the fibers, as shown in Fig. 3. Figure 4 illustrates a semi-quantitative mapping of Ti in the cross section of the same fiber as in Fig. 3 perpendicular to the growth direction. The Ti distribution map clearly displays striations showing a coaxial ring pattern of concentration variations in the fiber cross section. The number

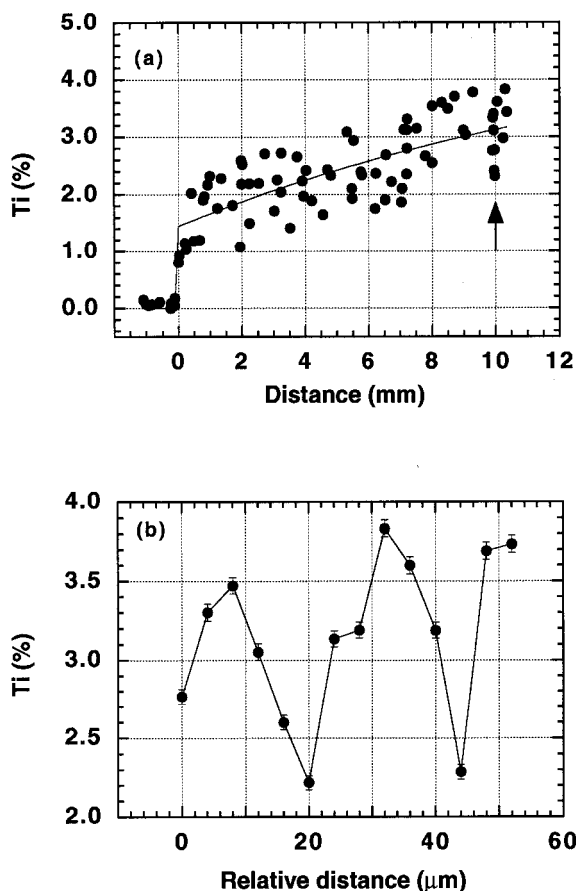


Fig. 2. Variation of Ti concentration along the growth direction in a YAG fiber: (a) macroscopic distribution, (b) microscopic fluctuations near the point indicated by the arrow in Fig. 2(a).

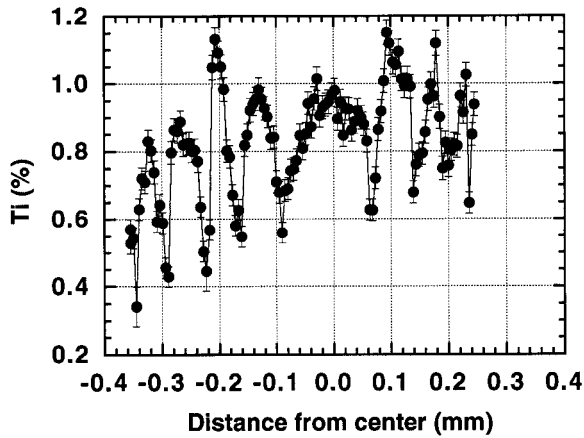


Fig. 3. Ti-distribution across the diameter of a grown YAG fiber.

of rings found in Fig. 4 is reasonable, assuming a fluctuation spacing of 20–30 μm along the growth direction and the simple convex growth interface having a height of 200–300 μm [6]. This pattern of dopant distribution suggests that periodic fluctuations occur in the growth rate and/or the dopant concentration in the melt.

Striations, typically observed in Czochralski-grown crystals, are correlated with crystal rotation and melt convection [7,8]. In the LHFZ method, perturbations such as irregular melting of the feed rod, which leads to a change in zone volume, may also induce these fluctuations. The irregular melting is believed to be influenced primarily by misalignment of the feed rod, seed crystal and laser beams. Under

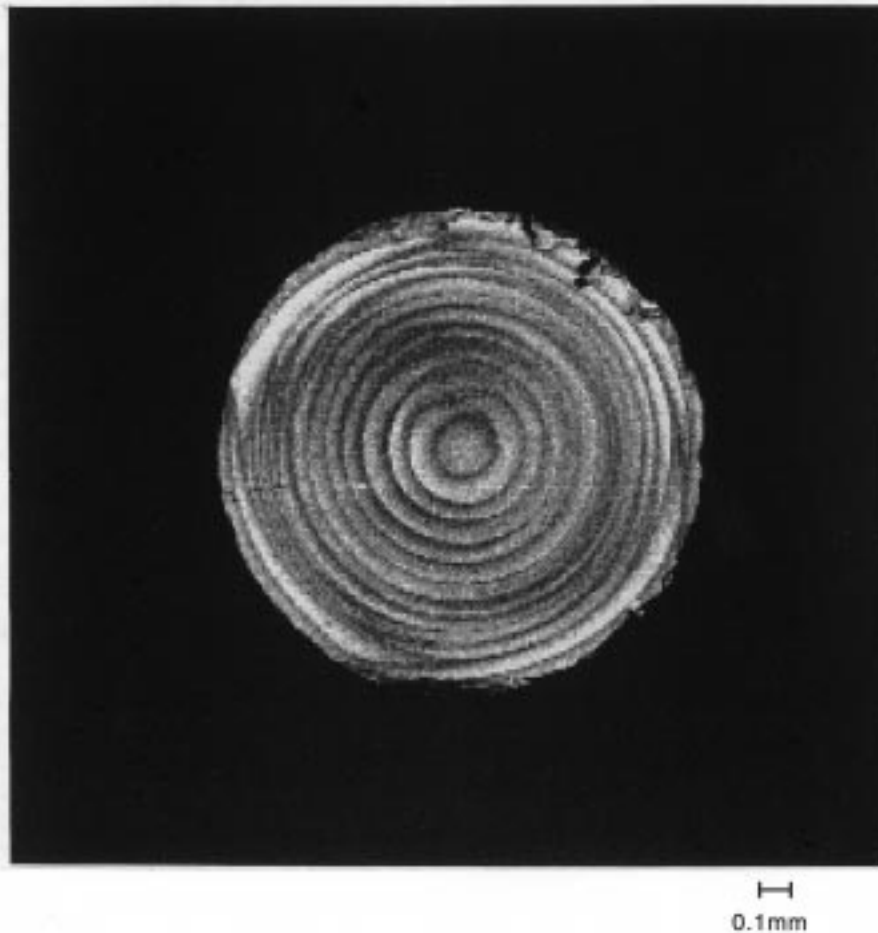


Fig. 4. 2-dimensional mapping of Ti in the radial cross-section of the same YAG fiber as in Fig. 3. The lighter the color, the higher the Ti concentration.

these circumstances, fluctuation cycles should be correlated with feed/seed rotation rates. Irregular melting also occurred due to non-uniform heating when feed rods with square cross-section were used [9].

The typical fluctuation wavelengths observed in most fibers are consistent with estimates based on the assumption of single growth interval completed during each rotation of the fiber or the feed rod (e.g., 16 μm and 21 μm for rotation rates of 21 rpm and 16 rpm, respectively). Therefore, the fiber/feed rotation rate during growth is likely to be one of the major factors contributing to these fluctuations.

In order to further investigate this correlation with fiber rotation, we grew a Ti-doped fiber where the crystal rotation rate was changed from a typical rate of 21 rpm to 0 rpm in the course of growth, while the feed rod was being rotated at a constant rate of 16 rpm. Figure 5 shows the fluctuations in Ti concentration in the regions grown at the rotation rate of 21 rpm and in those with no rotation of the fiber. The magnitude of the fluctuation in the no-rotation region was reduced to about 50% of that in the crystal grown at the rotation rate of 21 rpm, as summarized in Table 2. As for the peak-to-peak distance, the no-rotation fiber seems to have a more regular fluctuation, as shown in Fig. 6. The concentration varies with an approximately 21 μm interval. It is worth noting that this interval coincides with the growth length (21 μm) during one rotation of the feed rod. Hence, the feed rotation also seems

Table 2. Effect of crystal rotation on Ti dopant concentration (x in %) (at constant feed rotation of 16 rpm)

| Crystal rotation rate | | 21 rpm | 0 rpm |
|-----------------------|---------------------|--------|-------|
| Ti (%) | Minimum | 3.388 | 3.684 |
| | Maximum | 4.914 | 4.420 |
| | Mean | 4.246 | 4.082 |
| | Avg. Peak-to-Valley | 0.993 | 0.463 |

to affect the fluctuation in the case of no-crystal rotation.

Post-growth annealing of Ti-doped fibers was initiated with the intention of investigating the possibility of reducing the spatial composition modulation by diffusion. Anneals were performed at 1550°C for 24 h in 0.1% CO_2/CO ($\text{PO}_2 = 8 \times 10^{-14}$ atm) mixed gas. Although surface precipitation of Ti-rich phases was seen, no changes in the microscopic distribution of Ti in the fiber were observed under these conditions (see Fig. 7). On this basis, the diffusion coefficient of Ti was estimated to be less than 10^{-12} cm^2/s at 1550°C.

4. Conclusion

An electron probe microanalysis (EPMA) of Ti-doped YAG fibers grown by the LHFZ process revealed fluctuations in Ti concentration of up to 30% relative to the mean at spacings of the order of 20 μm along the growth direction. The wavelengths of major

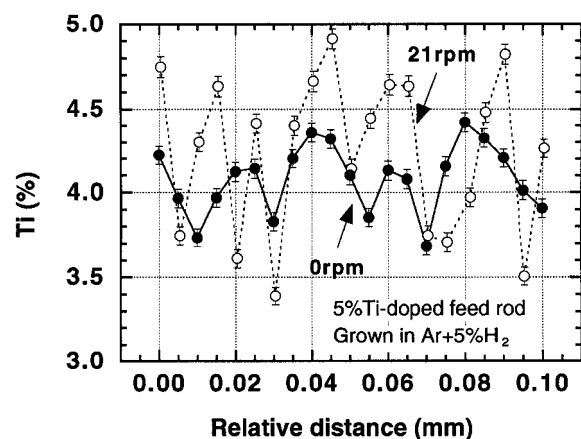


Fig. 5. Fluctuations of Ti concentration along the growth direction in the regions where the fiber rotation-rates were 21 rpm and 0 rpm.

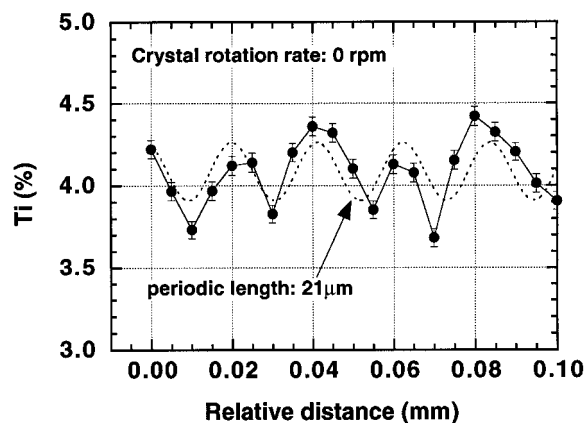


Fig. 6. Variation of Ti concentration in a YAG fiber grown without crystal rotation. The broken line indicates a sine curve with a periodic length of 21 μm .

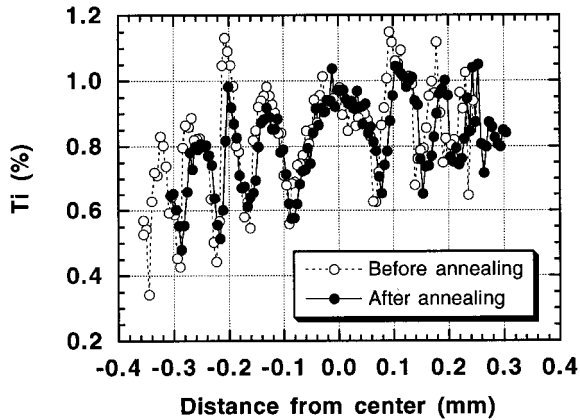


Fig. 7. Ti-distributions across the diameter of the same fiber as in Fig. 4 before and after annealing at 1550°C for 24 h.

microscopic fluctuations (16 and 21 μm) observed in this study appear to be related to the growth length during each rotation of the feed rod and fiber, respectively. Although the mechanisms remains unclear, asymmetric heating about the rotational axes resulting from misalignment of the feed rod and fiber relative to the laser beams is suggested as the most likely source. The spatial fluctuations in Ti concentration remained unchanged after annealing at 1550°C for 24 h, suggesting that the diffusion coefficient of Ti in YAG is below 10^{-12} cm^2/s .

Acknowledgment

This work was supported by an AT&T Bell Laboratory Fellowship (J.K.W.C.) and Sumitomo Electric Industries, Ltd. We would like to thank Dr. J.S. Haggerty and Dr. J. Sigalovsky for useful discussions on crystal growth and the use of the laser growth systems. We also acknowledge the assistance of Drs. Michael J. Jercinovic and Nilanjan Chattenjee with the EPMA measurements.

References

1. R.S. Feigelson, *J. Crystal Growth*, **79**, 669 (1986).
2. J.S. Haggerty, K.C. Wills, and J.E. Sheehan, *Ceram. Eng. Sci. Proc.*, **12**, 1785 (1991).
3. J. Sigalovsky, J.S. Haggerty, and J.E. Sheehan, *J. Crystal Growth*, **134**, 313 (1993).
4. S.R. Rotman, M. Roth, H.L. Tuller, and C. Warde, *J. Appl. Phys.*, **66**, 1366 (1989).
5. J.K.W. Chen, *The Electrical and Optical Properties of Doped Yttrium Aluminum Garnets*, Ph.D Thesis, Department of Materials Science and Engineering, MIT, Cambridge, MA, USA (1994).
6. T. Kotani, J.K.W. Chen, and H.L. Tuller, *J. Electroceramics*, to be published.
7. A. Murgai, H.C. Gatos, and A.F. Witt, *J. Electrochem. Soc.*, **123**, 224 (1976).
8. A.F. Witt, M. Lichtensteiger, and H.C. Gatos, *J. Electrochem. Soc.*, **120**, 1119 (1973).
9. C.T. Yen, D.O. Nason, and W.A. Tiller, *J. Mater. Res.*, **7**, 980 (1992).